01 Mar 1984

Preparation And Characterization Of Composite Hollow Fiber Reverse Osmosis Membranes By Plasma Polymerization. 1. Design Of Plasma Reactor And Operational Parameters

P. J. Heffernan

K. Yanaglhara

Y. Matsuzawa

E. E. Hennecke

et. al. For a complete list of authors, see https://scholarsmine.mst.edu/chem_facwork/3503

Recommended Citation

P. J. Heffernan et al., "Preparation And Characterization Of Composite Hollow Fiber Reverse Osmosis Membranes By Plasma Polymerization. 1. Design Of Plasma Reactor And Operational Parameters," *Industrial and Engineering Chemistry Product Research and Development*, vol. 23, no. 1, pp. 153 - 162, American Chemical Society, Mar 1984.
The definitive version is available at https://doi.org/10.1021/i300013a031

α = probability of chain propagation
ϑ_i = coverage (fraction of saturation density) of species i
$\kappa = (k_{tp}/k_{to})K_3^{0.5}$
$\lambda = (K_3^2K_5K_6K_7K_8)/(K_2k_4)$
$\mu = (k_pK_1K_3^{2.5}K_5^2K_6^2K')/(K_2k_4)$
$\nu = (k_pK_1K_3K_5K_6)/k_{to}$
$\rho = (K_3^2K_5K_6K_7)/K_1$

Registry No. Carbon monoxide, 630-08-0; ruthenium, 7440-18-8.

Literature Cited

Batchelder, R. F.; Penniine, H. W.; Schehl, R. R. Technical Publication DOE/PETC/TR-83/6, U.S. Dept. of Energy, Pittsburgh, PA, April 1982.
Biloen, P.; Sachtler, W. M. H. *Adv. Catal.* **1981**, *30*, 165-216.
Brady, R. C., III; Pettit, R. *J. Am. Chem. Soc.* **1980**, *102*, 6181-2.
Brady, R. C., III; Pettit, R. *J. Am. Chem. Soc.* **1981**, *103*, 1287-9.
Cant, N. W.; Bell, A. T. *J. Catal.* **1982**, *73*, 257-271.
Carberry, J. J. "Chemical and Catalytic Reaction Engineering"; McGraw-Hill: New York, 1976.
Dalla Betta, R. A.; Piken, A. G.; Shelef, M. *J. Catal.* **1974**, *35*, 54-60.
Dry, M. E. "Catalysis. Science and Technology"; Springer-Verlag: Berlin, West Germany, 1981.
Fajula, F.; Anthony, R. G.; Lunsford, J. H. *J. Catal.* **1982**, *73*, 237-256.
Kellner, C. S.; Bell, A. T. *J. Catal.* **1981a**, *71*, 296-307.
Kellner, C. S.; Bell, A. T. *J. Catal.* **1981b**, *70*, 418-432.
Polizzotti, R. S.; Schwarz, J. A. *J. Catal.* **1982**, *77*, 1-15.
Storch, H. H.; Golumbic, N.; Anderson, R. B. "The Fischer-Tropsch and Related Syntheses"; Wiley: New York, 1951.
Takoudis, C. G. *J. Catal.* **1983**, *79*, 281-5.
Vannice, M. A. *J. Catal.* **1975**, *37*, 462-473.
Vannice, M. A. *Catal. Rev. Sci. Eng.* **1976**, *14*, 153-191.
Weller, S. *AIChE J.* **1956**, *2*, 59-62.

Received for review August 22, 1983
Accepted September 26, 1983

This work was partially supported by CONOCO, Inc., and NALCO Chemical Company through grants to the Purdue Coal Research Center.

Preparation and Characterization of Composite Hollow Fiber Reverse Osmosis Membranes by Plasma Polymerization. 1. Design of Plasma Reactor and Operational Parameters

P. J. Heffernan, K. Yanagihara, Y. Matsuzawa, E. E. Hennecke, E. W. Hellmuth, and H. Yasuda*

Department of Chemical Engineering and Graduate Center for Materials Research, University of Missouri—Rolla, Rolla, Missouri 65401

Composite hollow fiber reverse osmosis membranes were prepared by depositing a thin layer (10–50 nm) of plasma polymers on hollow fibers with porous walls (made of polysulfone). The coating was carried out in a semicontinuous manner with six strands of substrate fibers. Operational parameters which influence reverse osmosis characteristics of composite membranes were investigated.

Introduction

Thin film formation which occurs in glow discharge of organic vapors is generally referred to as "glow discharge polymerization" or "plasma polymerization". Polymers formed by plasma polymerization of a monomer (e.g., styrene) are considerably different from the polymer formed from the same monomer by conventional polymerization processes. Furthermore, many organic compounds which are not considered as monomers for polymerization can be polymerized by plasma polymerization. In many cases, plasma polymers (polymers formed by plasma polymerization) are prepared in networks of highly branched and highly cross-linked segments. Polymers deposit onto a substrate material placed in glow discharge from low-pressure plasma (partially ionized state of vapor). Because of interaction of plasma with the substrate polymer and of the unique mechanisms of polymer formation, excellent adhesion of a thin deposit to the substrate can be obtained. Typical plasma polymers are commonly amorphous and thin films without macroscopic pinholes can be readily obtained.

Because of these advantageous features of plasma polymerization, an ideal composite reverse osmosis membrane can be prepared by plasma polymerization if the right selection of porous substrate and the proper execution of plasma polymerization are combined. The potential use of plasma polymerization for membrane preparation has been demonstrated in several papers published in recent years (Buck and Davar, 1970; Hollahan and Wydeven, 1973; Yasuda et al., 1973(a), 1975, 1976; Bell et al., 1975), and some noteworthy unique characteristics of plasma polymerized membranes have also been reported (Yasuda and Lamaze, 1973a): for example, (1) very stable performance independent of salt concentration and applied pressure; (2) salt rejection and water flux both increase with time in the initial stage of reverse osmosis resulting in improvement of reverse osmosis membrane performances with the time of operation; (3) high salt rejection (over 99%) with high water flux (up to 38 gfd) obtained with 3.5% NaCl salt solution; and (4) the prepared membranes were chemically durable.

On the other hand, however, all membranes by plasma polymerization are prepared in relatively small laboratory scale batch processes, and data available are insufficient to judge the true practicability of the method in large-scale applications. Many practitioners of membrane technology, with lack of fundamental knowledge about the method, have failed to recognize the potential of plasma polymerization in membrane preparation. The most frequently raised questions, or expressions of doubt about the practicability of the method, are concerned with (1) reproducibility of the process and (2) difficulty of scale-up for a continuous operation. Therefore, the major objectives of this study are focused on these two factors.

In order to investigate the reproducibility and the feasibility of continuous operation, semicontinuous plasma polymerization utilizing hollow fibers as substrates was chosen and a special tandem reactor was constructed.

0196-4321/84/1223-0153$01.50/0

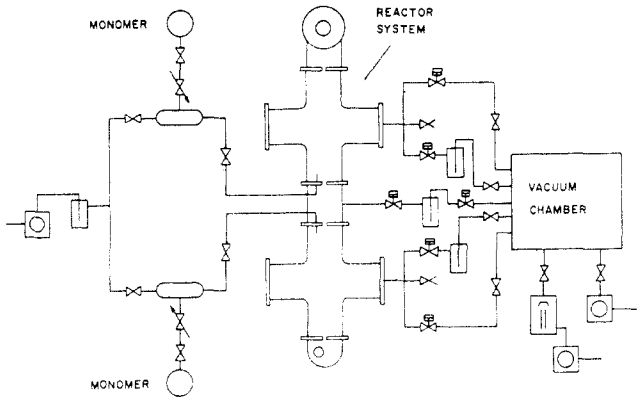

Figure 1. Plasma reactor system.

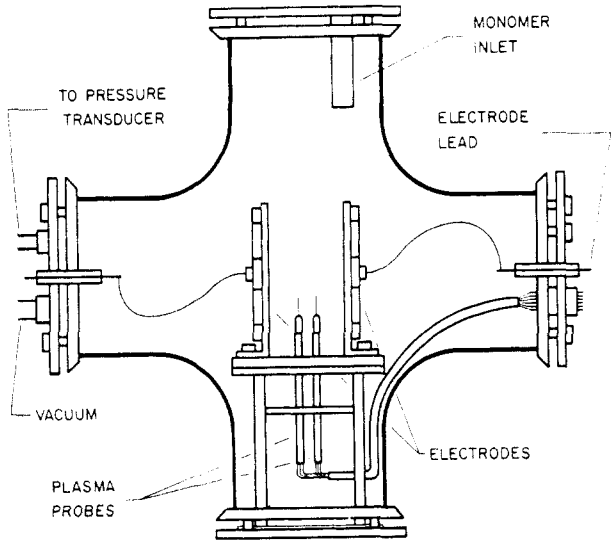

Figure 2. Schematic of a single reactor.

Factors which influence the continuous plasma polymerization are examined in this study.

Experimental Section

A. Plasma Reactor System. The reactor system used in this work is illustrated in Figure 1.

1. General. It consists of two glass reaction vessels in series, each containing a pair of circular stainless steel electrodes. The two reactors are separated by a highly evacuated buffer chamber, which ensures that there is no cross-contamination of gas between reactors. The fiber is stored in six spools at the bottom of the reactor system. From these spools, six fibers are drawn upward between the electrodes by a motor driven take-up roll at the top of the equipment. The fibers pass from one chamber to another through narrow Teflon slits in the plates separating the chambers.

Each reactor is linked to a separate monomer feed system which can be evacuated via the monomer vacuum pump. Monomer purification can thus be achieved without disturbing the reactor system.

An MKS Baratron Type 170 pressure meter is connected to each reaction chamber. These instruments are capable of measuring vacuum in the range of 10^{-3}–1 torr independent of gas nature or composition.

2. Reactor Geometry. A schematic of a single plasma reaction vessel is shown in Figure 2. The reactor has a volume of approximately 23 L. The electrodes are 13.2 cm in diameter and are positioned 6.2 cm apart. Magnetic enhancement is used to confine the glow discharge to the region between the electrodes. This is achieved by first attaching an iron ring concentrically to the back of each electrode. A small iron disk is then fixed to the electrode center so that eight bar magnets can be placed at the back of the electrode with north poles on the ring and south poles on the disc. Two plasma probes are located in the interelectrode region to monitor plasma parameters.

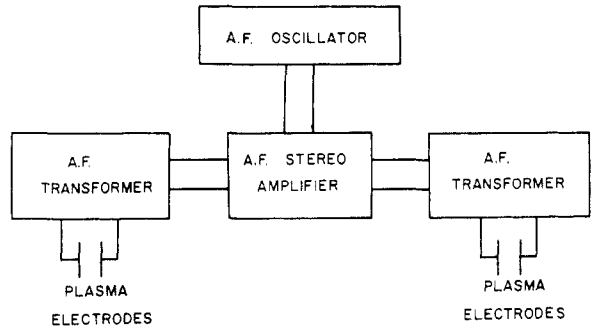

Figure 3. Audio frequency power supply system.

3. Power Supply Systems. The plasma reactors can be operated over a range of frequencies from low-frequency alternating current (ac) to radio frequency (RF). however, in the present work, an audio frequency of 10 kHz was employed. The power supply system used is shown in Figure 3.

The AF power system consists of a Hewlett-Packard AF oscillator, Model 200CD, connected to an AF stereo amplifier. The amplifier is a Crown Model DC 300A unit. Each of the two output channels is connected to an NWL AF transformer, Model 24617, which steps up the output voltage to about 500 V. The secondary winding on each of these transformers is connected directly to a pair of plasma electrodes.

B. Reverse Osmosis Unit. The hollow fiber membranes are tested in a high pressure recirculation loops as shown in the simplified flow diagram of Figure 4. The feed solution storage tank contains synthetic saline water consisting of a solution of table salt in tap water. A Milton Roy high-pressure positive displacement pump, Model C, is used to pump the feed solution under pressure through the cells. A hydraulic accumulator minimizes pressure flucutations in the lines and small particles in the feed solution are removed by a water sediment filter mounted between the pump and the reverse osmosis cells. Fluid pressure in the unit is indicated by Bourdon pressure gauges. A stainless steel Grove pressure regulator controls the operating pressure of the system in accordance with the nitrogen gas pressure supplied to the dome of the regulator. The nitrogen gas is available from commercial gas cylinders. High-pressure 316 stainless steel tubing and fittings were used throughout the system to minimize corrosion.

The reverse osmosis cells are an arrangement of eight equal lengths of $^1/_2$-in. nominal stainless steel pipe placed in series, into which eight potted fiber samples can be inserted. The salt water flow is in a direction parallel to the fibers with a velocity which can be as high as 27 cm/s, if the water pump is operated at maximum flow capacity (93.0 gph).

A practical consideration to be borne in mind when testing hollow fiber reverse osmosis membranes is that the large membrane packing ratio can sometimes lead to severe membrane polarization. The analysis of Sherwood et al. (1965) can be used to determine the increase in effective osmotic pressure due to salt concentration at the membrane boundary. For a flow velocity of 27 cm/s (the maximum attainable with the reverse osmosis loop), the ratio of the salt concentration at the membrane to the bulk salt concentration is estimated to be 1.25. this change is

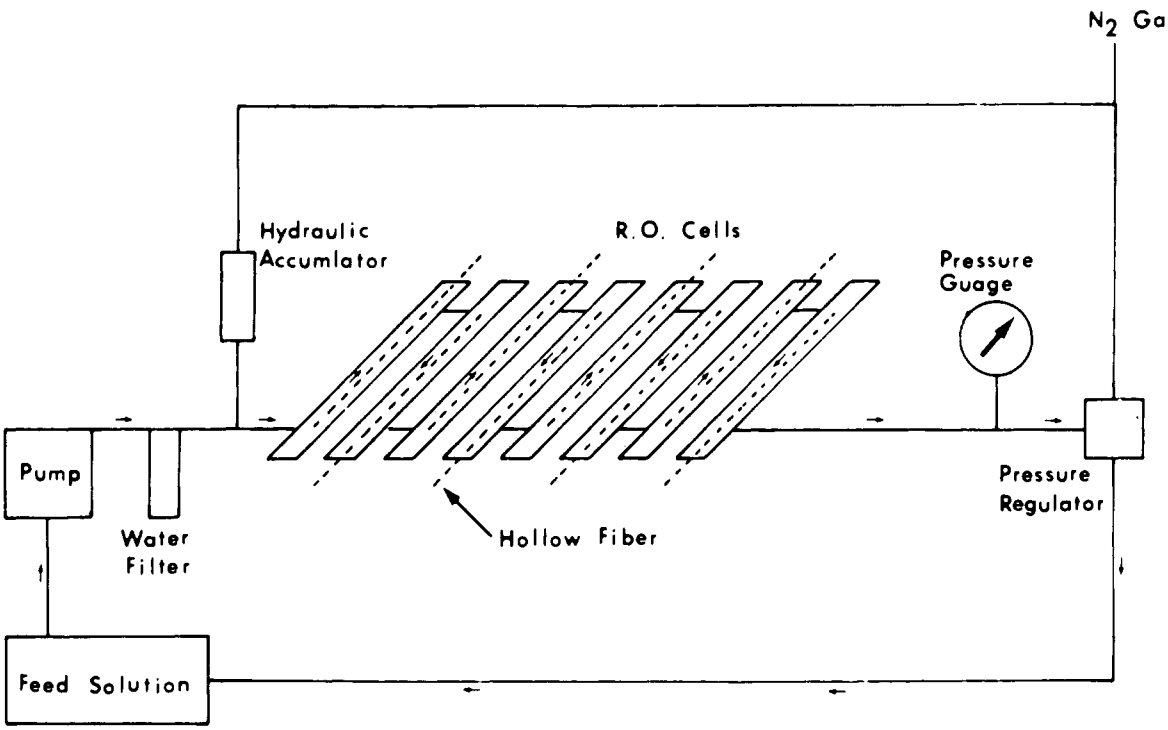

Figure 4. Flow diagram of reverse osmosis test equipment.

quite small in comparison to the driving pressure (1300 psi) so that polarization effects are minimal.

C. Product Water Analysis. The sodium chloride concentration in the feed solution and permeate were measured with a Radiometer conductivity meter, Model CDM 2e. The percentage salt rejection is defined as

(salt concentration of feed) − (salt concentration of permeate)/(salt concentration of feed)

The membrane water flux of a hollow fiber sample was calculated in units of gfd (gallons/ft^2 day) from the quantity of permeate collected over a given period of time.

Results and Dicussion

A. Hollow Fibers. Porous polysulfone in the form of hollow fibers was prepared and supplied through the courtesy of FRL, Dedham, MA. The fibers have an outside diameter of approximately 0.25 mm and an inside diameter of 0.09 mm. Prior to coating these fibers, it was decided to carry out an investigation of their susceptibility to damage. An attempt was also made to determine the distribution of pore sizes on the fiber surface.

An electron micrography of the surface of a polysulfone fiber appears to be smooth except for small scratch-like marks. At magnifications of 5000 and 40 000 there is no visible sign of surface pores. If the magnification is increased to 70 000, the surface still remains smooth, indicating that the diameter of the surface pores is less than 500 Å. This substrate is very suitable for the deposition of a plasma polymer membrane since small pore size allows a very thin coating to be used to cover up the pores, while at the same time offering a low resistance to water flux through the membrane.

Electron micrographs were also prepared of fibers which were dried after removal from water and methanol. No significant differences were observed between fibers which were dried slowly and those dried rapidly. It is possible, however, that changes in surface pore size can occur, but this was not observed within the limits of magnification available for the equipment used (70 000×).

Tests were carried out to determine the extent to which the hollow fibers might be damaged by abrasion against surfaces during their passage through the reactor or by handling. Electron microscopy was again used to determine the surface condition of the fibers. It was found that stretching the fibers and rubbing them against Teflon surfaces similar to those in the reactor system had no effect. Handling of wet fibers was also found to cause no problems, but if dry fibers were handled, the surfaces could be significantly damaged. In view of this, it was decided to handle the fibers by using plastic gloves only.

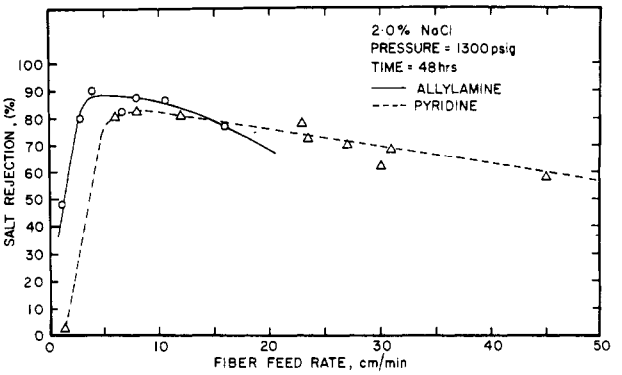

Figure 5. Salt rejection vs. fiber feed rate for allylamine and pyridine plasma polymer coatings. The monomer flow rate and initial discharge current were 14.0 cm^3(STP)/min and 105 mA, respectively. The initial reactor pressure was 17.4 mtorr.

B. Reverse Osmosis Membranes Prepared with Different Monomers. Three nitrogen-containing compounds were selected as monomers for plasma polymer coating. These were pyridine, allylamine, and monomethylamine. Pyridine and allylamine were chosen because previous work has shown that they produce useful membranes (Peric et al., 1977; Morosoff, 1978). Monomethylamine was tested as an alternative nitrogen compound. In all experiments, only the lower reactor was used for plasma deposition. Reverse osmosis results obtained with monomethylamine were not very encouraging.

Figures 5 and 6 show the variation in salt rejection and water flux with fiber feed rate through the plasma reactor for pyridine and allylamine plasma polymer coatings. As

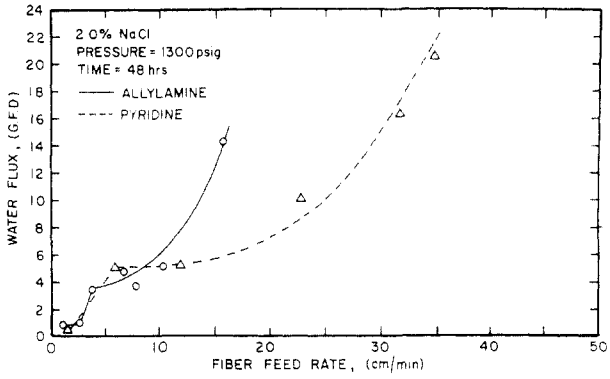

Figure 6. Water flux vs. fiber feed rate for allylamine and pyridine plasma coatings. The monomer flow rate and initial discharge current were 14.0 cm^3/(STP)/min and 105 mA, respectively. The initial reactor pressure was 17.4 mtorr.

the fiber speed is reduced, the thickness of the plasma polymer coating increases. Pores on the fiber are gradually covered over with the result that salt rejection increases steadily while the water flux decreases. The fact that the salt rejection increases slowly as the fiber speed is reduced would seem to indicate that there is a large distribution of pore sizes on the fiber surface. In the case of pyridine, a maximum salt rejection of 83% is obtained at a fiber speed of 8 cm/min. For allylamine, the maximum salt rejection is 92%. This occurs at a fiber feed rate of 4 cm/min. The difference in fiber feed rate corresponding to a maximum salt rejection reflects the fact that the deposition rate of allylamine is about half that of pyridine under similar reaction conditions (Yasuda, 1973b). Polymer deposition rate measurements carried out for allylamine show that the deposited polymer thickness is about 200 Å at this stage.

A further decrease in the fiber feed rate causes both the salt rejection and water flux to decline steeply, indicating a major change in the plasma polymer coating or the substrate. The reason for this is not clear at present. Cracking of the deposited coating alone due to a buildup of internal stress has to be ruled out since this would lead to an increase in water flux. Complete coverage of the surface pores on the fiber with plasma polymer does not offer an explanation either. A reduction in water flux would be expected due to a change in the transport mechanism through the membrane. However, the salt rejection should not decrease.

If one considers possible changes which might take place in the substrate, an explanation for the observed behavior can be postulated. Degradation of the porous fiber can occur due to bombardment by energetic particles present in the plasma and to ultraviolet irradiation produced by the plasma. The ultraviolet radiation should be able to penetrate through the polymer coating even for thicknesses of several hundred angstroms.

Substrate degradation can also result from heat generated by the plasma and from the adsorption of monomer on the substrate. It has been observed that pyridine dissolves the polysulfone fiber, whereas allylamine causes it to contract.

If decomposition of the fiber is severe (as can occur for long coating periods), it can lead to changes in pore size. This in turn would alter the transport properties of the substrate and probably reduce it water permeability. Degradation of the fiber surface might also affect the adhesion of the plasma polymer layer to the fiber.

As the thickness of the plasma polymer membrane increases, cracks can form resulting in a decrease in salt rejection. Thus, the combined effect of substrate degradation and the formation of cracks in the membrane coating can produce a fiber with low salt rejection and water flux.

It is interesting to consider the results of experiments carried out in which the monomer was allowed to adsorb on the substrate for some time prior to plasma polymerization. It was found that these membranes exhibited very low flux and salt rejection.

Figures 5 and 6 suggests a number of comparisons between the monomers allylamine and pyridine. For allylamine: (1) salt rejection increases more steeply with decreasing fiber feed rate; (2) the water flux increases steeply with increasing fiber feed rate; (3) at maximum salt rejection, the water flux is lower than that for pyridine.

The decrease in salt rejection and increase in water flux with increasing fiber feed rate, observed at high fiber feed rates, are due to incomplete coverage of fiber surface pores with plasma polymer. The steep slope observed in the case of allylamine suggests that the pore-filling process is efficient and that the polymer film is nonporous. The lower water flux at maximum salt rejection for allylamine further indicates that a high density is achieved in the coating.

An important conclusion which can be made at this stage is that there is a critical coating thickness above which deterioration of the desalination characteristics occurs. It can be postulated that this critical thickness depends only on the pore size distribution of the fiber surface and its susceptibility to degradation in the plasma.

The maximum salt rejection, which occurs at the critical thickness, depends on the monomer, coating conditions, and the substrate nature. Because of this, it cannot be concluded the pyridine is not as good a monomer as allylamine for preparing reverse osmosis membranes by plasma polymerization. However, the data available suggested that allylamine was the more suitable monomer for use in further research. For this reason, all subsequent experiments were carried out with allylamine plasma polymer coatings.

A dye staining technique was used to confirm the presence and uniformity of the plasma polymer coating. The dye was DuPont textile identification stain no. 4. Uncoated fibers are stained dark brown while coated fibers have a staw-like coloration. An optical microscope was used to examine the fibers. The coating appears to be coherent and free of macroscopic pinholes.

C. Thickness of Coating on Hollow Fibers. The existence of a critical coating thickness for optimum desalination properties suggested that a series of experiments be carried out to measure deposition rates of plasma polymerized allylamine. The measurements were made for a number of different monomer flow rates and electrode current settings.

The results were used to plan further hollow fiber coating experiments that would test the effect of different monomer flow rates and discharge currents on membrane performance. This was done under the assumption that equal polymer coating thicknesses would give fibers of near equal desalination properties—the difference being accounted for by change in the chemical and/or structural characteristics of the coating and substrate.

The deposition rates were determined by depositing the plasma polymer on small pieces of aluminum foil placed along a parallel plane lying midway between the two electrodes. (For deposition rate calculations, it is assumed that the density of allylamine plasma polymer is 1.30 g/cm^3.) These data are presented in Figures 7, 8, and 9.

The deposition rates thus obtained by inserting stationary substrates reflect the distribution of plasma energy

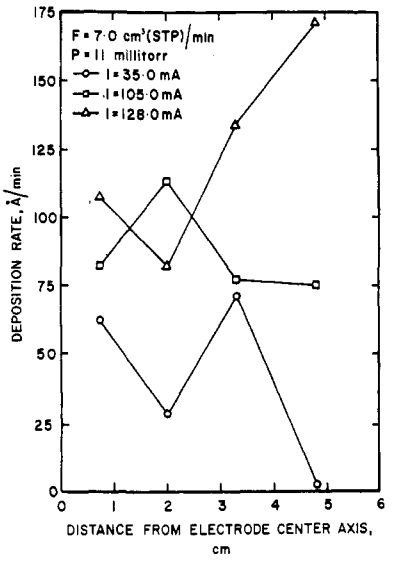

Figure 7. Polymer deposition rate profiles for a monomer flow rate of 7.0 cm^3(STP)/min.

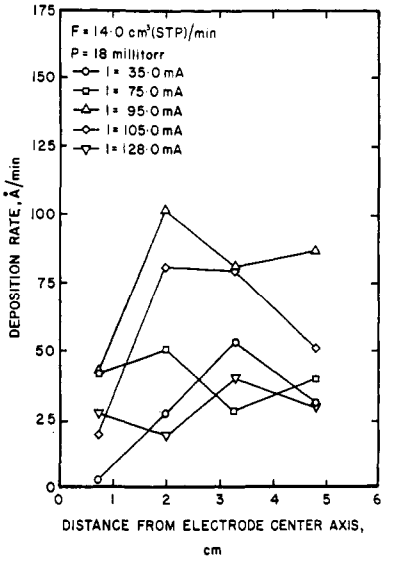

Figure 8. Polymer deposition rate profiles for a monomer flow rate of 14.0 cm^3(STP)/min.

density in the interelectrode space where the substrate fibers travel during the coating operation. The magnetic enhancement of low-pressure plasma generally results in a doughnut shape intense glow close to the surface of the electrode. This is one of the advantageous characteristics of the magnetron plasma of which the plasma can be contained in the interelectrode space in a low-pressure operation, resulting in a higher deposition rate (Morosoff, 1978; Cormia et al., 1977). On the other hand, the uneven plasma energy density yields uneven distribution of deposition rates in the interelectrode space. However, these uneven local deposition rates do not cause major problems in obtaining uniform coating thickness when moving substrates, such as fibers, are employed. Based on the deposition rate profiles shown in Figures 7, 8, and 9, and considering the geometrical symmetry in a circular electrode, the integrated deposition rate on each fiber can be calculated.

In the coating technique employed, six hollow fibers move simultaneously upward between the electrodes at a constant speed. A schematic of this arrangement is shown in Figure 10. deposition rate measurements were made at four locations between the electrodes. Using graphical integration, it is possible to relate these deposition rates

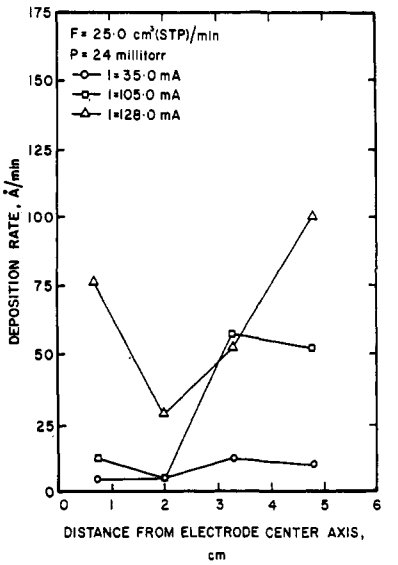

Figure 9. Polymer deposition rate profiles for a monomer flow rate of 25.0 cm^3(STP)/min.

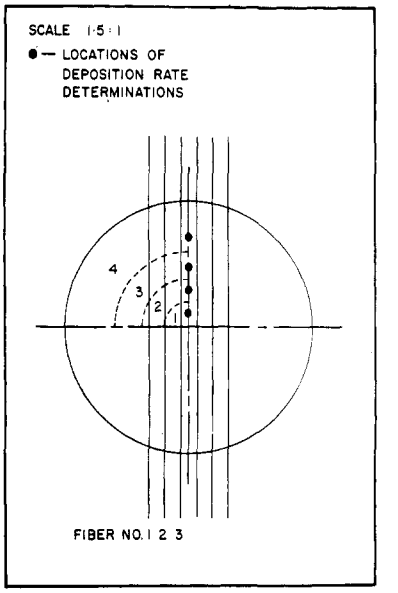

Figure 10. Schematic diagram showing the passage of hollow fibers between the discharge electrodes.

to the thickness of polymer deposited on each of the fibers. This procedure is described in the Appendix. The calculated coating thicknesses are shown in Table I for a series of reactor operating conditions.

It can be seen that the thickness of polymer deposited on each of the six fibers is approximately the same. This is largely due to the fact that the fibers are moving relative to the electrode system during coating. As each fiber moves between the electrodes, polymer is deposited at many different rates. The overall coating thickness reflects an average over all these values, and so it does not vary as much for each fiber as the localized deposition rates might suggest.

D. Factors Which Influence Continuous Operation. 1. Ambient Temperature of Plasma. When plasm polymerization was performed by using relatively high discharge power, the hollow fibers of polysulfone (with porous wall) broke, and it was found that it was impossible to coat hollow fibers at high discharge wattage. It was suspected that the breakdown of hollow fibers was due to excessive heating of fibers in plasma. It was also noticed that the reactor gradually warmed up during the process

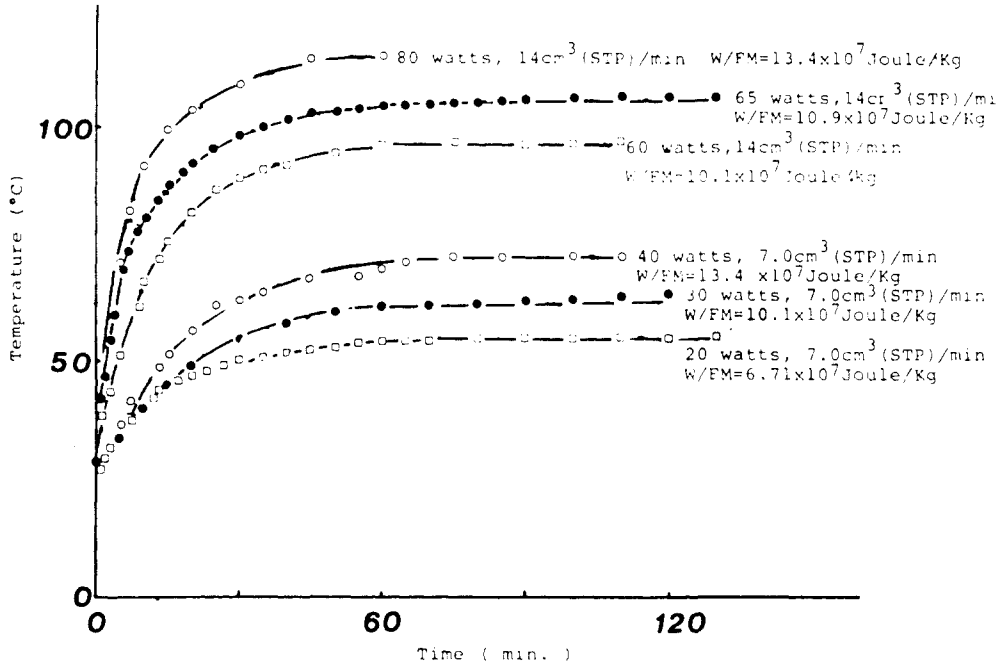

Figure 11. Temperature measurements of glow region with discharge time.

Table I. Effect of Fiber Position on Polymer Coating Thickness

flow rate, cm³(STP)/min	electrode current, mA	coating thickness, Å[a] fiber no. 1[b]	fiber no. 2	fiber no. 3
7.0	35.0	360	360	440
7.0	105.0	1066	1140	1140
7.0	128.0	1760	1720	1790
14.0	35.0	480	450	390
14.0	75.0	500	540	550
14.0	95.0	1120	1160	1080
14.0	105.0	840	870	770
14.0	128.0	390	390	400
25.0	35.0	110	100	90
25.0	105.0	1160	1180	1340
25.0	128.0	870	850	950

[a] For a fiber feed rate of 1.0 cm/min. It is assumed that the coating thickness is inversely proportional to fiber feed rate. [b] Due to symmetry, the fibers numbered 1, 2, and 3 need only be considered.

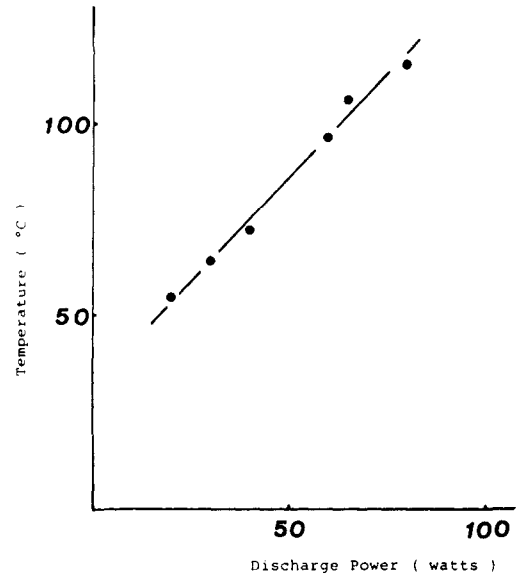

Figure 12. Relationship between temperature of glow region and discharge power.

of long-time operation. Therefore, it was decided to measure ambient temperature of glow discharge zone by placing a thermocouple. The results are summarized in Figure 11. The ambient temperature of plasma thus measured increases in the early stage of operation and reaches a steady-state value in 30 to 60 min, depending on the conditions of plasma polymerization. The steady-state value of temperature is directly proportional to discharge wattage as shown in Figure 12.

It is interesting to note that plasma polymerization is dependent on a composite parameter given by W/FM, where W is the discharge power, F is the monomer flow rate, and M is the molecular weight of the monomer (Yasuda and Hirotsu, 1978), as discussed in part 2 of this series of papers. The same value of W/FM can be obtained by various combinations of W and F. However, since ambient temperature of plasma is dependent on W alone, not on W/FM, the adverse effect of higher temperature can be avoided by selecting lower W and lower F to maintain the same level of W/FM.

Since the temperatures observed are not exceedingly high to melt polysulfone, the breaking of hollow fibers may be due to the irradiation effect of plasma, i.e., impinging ions and electrons, rather than the thermal effect. If this is the case, the cooling of electrodes may not contribute much to avoid breaking of fibers at high discharge wattage.

2. Drift of Voltage and Current Due to the Changes Which Occur at Electrode Surface. It should be noted that an electric discharge system which utilizes the confinement of electron by superimposed magnetic field (magnetron discharge) is used in this study. The advantages of using a magnetron discharge are as follows.

(a) Because of the confined plasma, it is possible to minimize the polymer deposition which otherwise occurs on undesired locations; e.g., walls of reactor. This factor is important for a long-time operation.

(b) It is possible to create plasma at much lower pressure by a magnetron discharge. Thus, it becomes possible to take advantage of low-pressure deposition, i.e., more uniform deposition and the high W/FM value without increasing W.

(c) It is possible to eliminate the deposition of polymers on a certain position of electrode (i.e., under the ring-

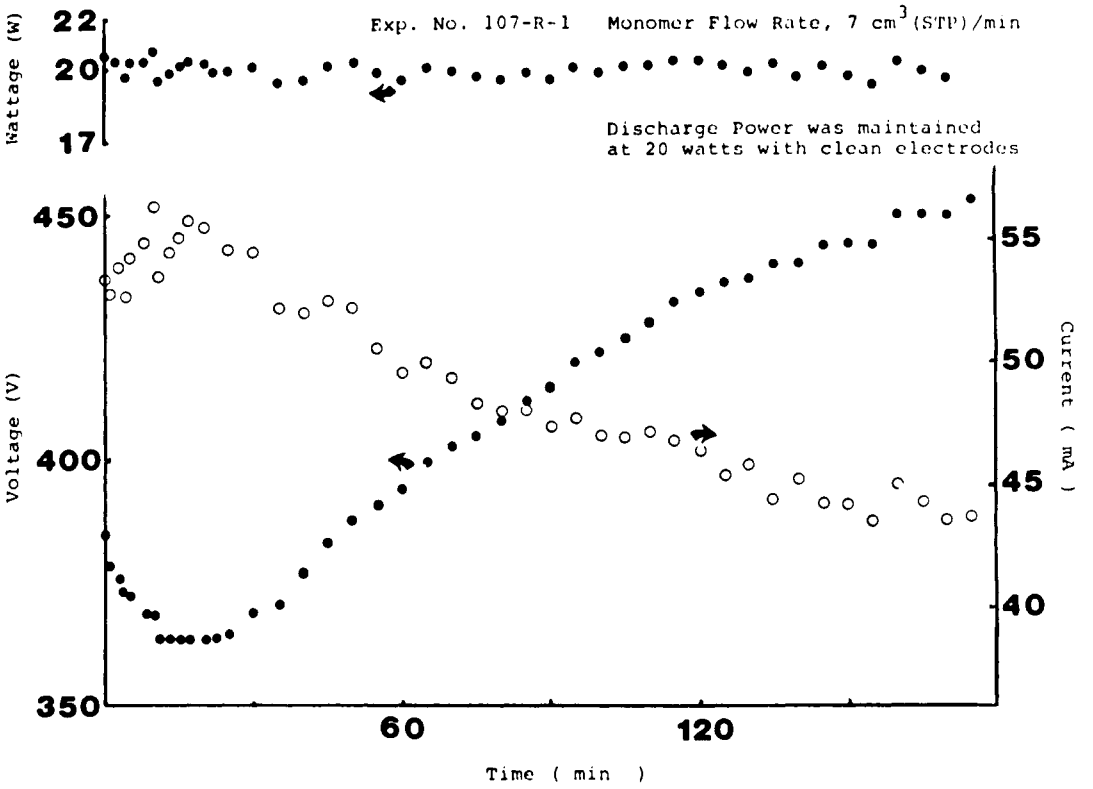

Figure 13. Electrical characteristics for glow discharge reaction vs. time.

shaped intense glow formed by a magnetron discharge). Thus, a long-time operation of a system becomes possible without being hampered by undesirable coating of electrode surfaces by plasma polymer.

All these factors are desirable in a continuous operation of plasma polymerization. On the other hand, these factors also point out that the most stable and reproducible plasma polymerization could be performed after the electrode surfaces have established a dynamic equilibrium with a continuously operating plasma.

The change of surface characteristics of electrodes can be visualized by the change of voltage and current to maintain a constant discharge wattage, as shown in Figure 13 when a clear electrode was used to start the run. The initial drop of voltage and increase of current are probably due to the increase of the temperature of the electrodes. According to the temperature measurement shown in Figure 11, the ambient temperature reaches a steady value within 30 min under this operating condition. The steady increase of voltage and steady decrease of current observed after the minimum (voltage) and the maximum (current) are due to the coverage of electrode surfaces by plasma polymer deposition. When a new experiment is carried out with electrodes used in the previous run under otherwise identical conditions, the discharge behaves as if it were a continuation of the previous run as shown in Figure 14. The initial changes at the high voltage and lower current compared to the clean electrodes are much smaller and the drift of voltage and current are much smaller during the period of 3 h. Steady voltage and current are reached after 2.5 h of operation.

When the conditions of plasma polymerization are changed, the electrodes which are conditioned in the previous runs under a different set of conditions undergo another process of establishing a new dynamic equilibrium with the new plasma polymerization conditions. One example of such a process is shown in Figure 15. In this case, higher wattage (high voltage and current) and a high monomer flow rate were used compared to the experiments shown in Figure 13 and 14. Furthermore, the discharge current rather than discharge wattage was maintained at a constant level. Under the constant current condition, the discharge voltage decreased during the initial period of 100 min and reached a steady value. Under this high current (wattage) discharge condition, the ablation which takes place at the electrode surface close to the intense glow ring is more pronounced and the uncoated area of electrode surface increases until a new steady state is established. The increase of exposed electrode area is manifested by the decrease of voltage to maintain a constant current level.

As shown in these data, the deposition of plasma polymer on the surface (a portion) of electrodes gradually changes glow discharge characteristics. The plasma probe measurement (measurement of electron temperature, T_e, and number of electrons, N_e) during the transient stage of discharge indicated that while no significant change in T_e is observed, a noticeable decrease of N_e is seen (Figure 16 and 17).

It is obvious from these observations that the best performance of plasma polymerization would be obtained after the system establishes a dynamic steady state, and such a steady state can be reached in a much shorter period of time if electrodes which are preconditioned in the environment of the actual operation are used. In other words, the best reproducibility of plasma polymerization can be obtained by a continuous operation. As pointed out by a recent study by Inagaki and Yasuda (1981), the beginning and the end of a batch plasma polymerization could cause other factors of variation, which are absent in a continuous process (except at the beginning of operation), since the substrate enters and leaves a steady state plasma.

Although during the transient period of operation, which varies less than 10 min to several hours, depending on the conditioning of the electrode surface, drift of voltage and current occurs, the reverse osmosis characteristics of plasma polymers are not much influenced by these changes in discharge conditions as long as the discharge power level

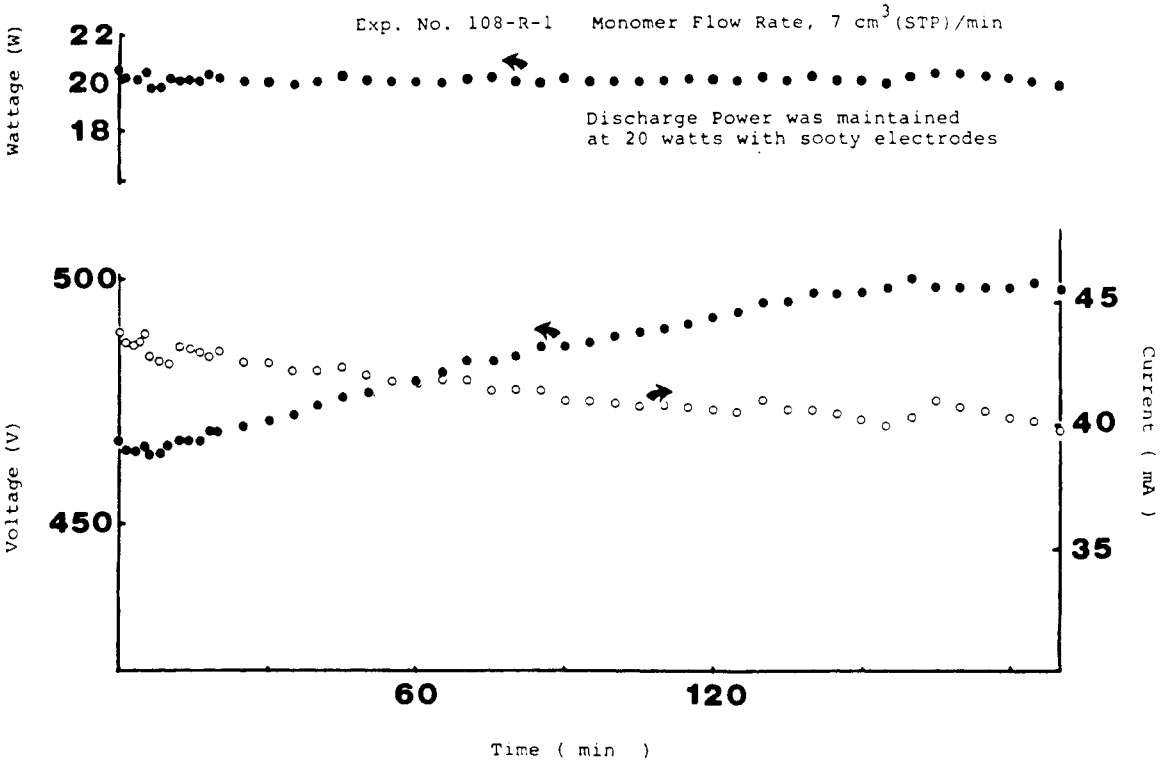

Figure 14. Electrical characteristics for glow discharge reaction vs. time.

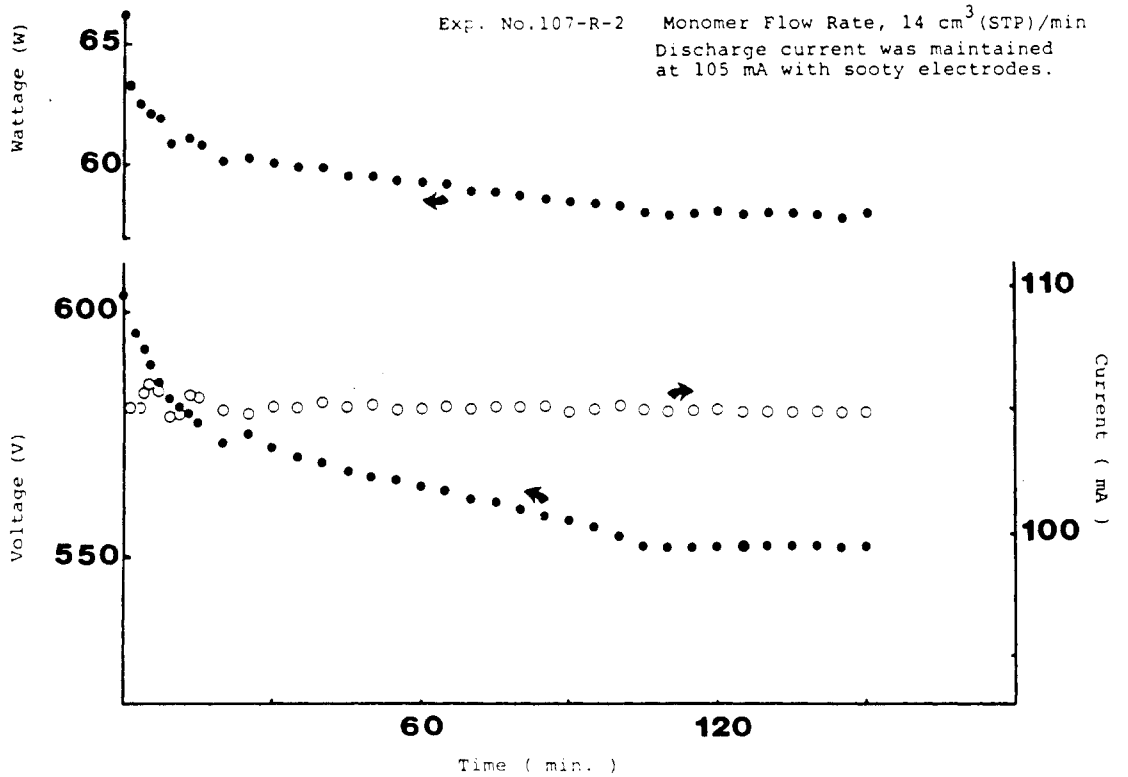

Figure 15. Electrical characteristics for glow discharge reaction vs. time.

is maintained above a threshold value.

We tried to control (1) discharge wattage and (2) discharge current during the transient stage of plasma polymerization; however, there was no significant difference between how the discharge is adjusted during this period. As shown in part 2 of this series of papers in which durability of membranes is discussed, the threshold value of W/FM appears to be more important, and as long as the W/FM value does not drift down below the threshold value during the transient stage, the variation in reverse osmosis characteristics of plasma polymers is small. In other words, the establishment of a dynamic equilibrium with respect to the state of electrode surface is more important than the adjustment of electric power input.

Conclusions

Plasma polymerization can be used to prepare hollow fiber composite membranes in a semicontinuous manner by passing hollow fibers through a plasma zone created by internal parallel electrodes.

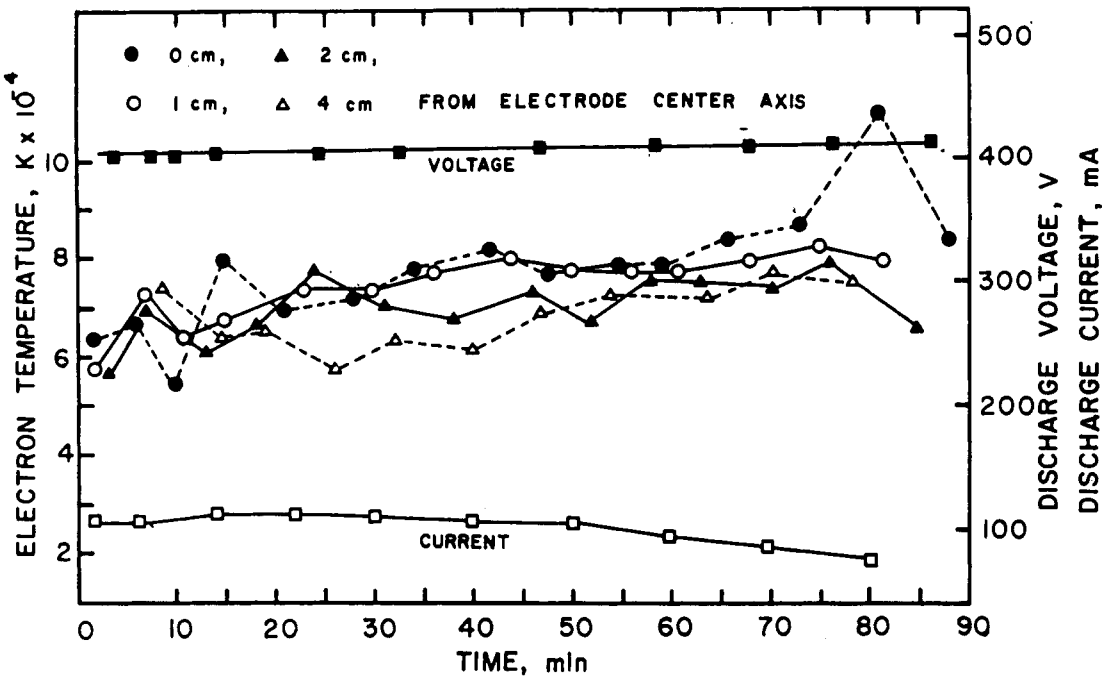

Figure 16. Time dependence profiles of voltage, current, and electron temperature (T_e) in an AF plasma without current control. The monomer flow rate and initial discharge current were 14.0 cm³ (STP)/min and 105 mA, respectively. The initial reactor pressure was 17.4 mtorr.

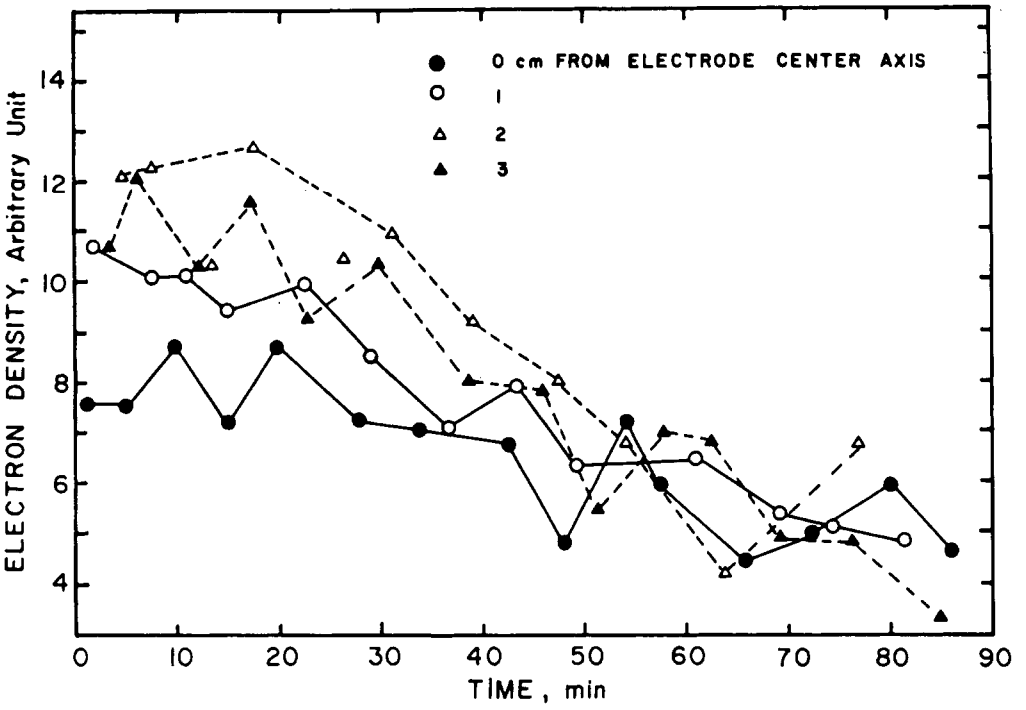

Figure 17. Time dependence profile of electron density (n_e) in an AF plasma without current control. The monomer flow rate and initial discharge current were 14.0 cm³(STP)/min and 105 mA, respectively. The initial reactor pressure was 17.4 mtorr.

Although the instantaneous deposition rates observed in different locations in the plasma zone are appreciably different, the overall deposition of a plasma polymer onto six strands of hollow fibers is uniform, and very little difference was found among fibers. This is an obvious advantage of continuously moving substrate employed in this arrangement.

There seems to be maximum thickness of plasma polymer layer, above which salt rejection and water flux both decrease as the coating thickness increases.

The establishment of a steady-state plasma seems to be the most important factor in obtaining reproducible results. In this respect, a semicontinuous process is ideal for the reproducible performance of plasma polymerization. The variation in operational parameters, such as discharge current, voltage, electron temperature, and number of positive ions, etc., becomes minimal as a steady-state plasma is established. The conditioning of electrode surface in the actual operational conditions plays an important role in the establishment of a steady state plasma.

Acknowledgment

This study was supported by the Office of Water Research and Technology, the U.S. Department of the Interior, under Grant No. 14-34-0001-8525.

Appendix

Calculated Thickness of Plasma Polymer Coatings. Described below is a method of calculating the thickness

of plasma polymer deposited on each of the six fibers as they move between the electrodes.

The calculations are based on experimental deposition rates at four locations in the interelectrode region. The deposition rates can be taken from the data shown in Figures 7, 8, and 9. It is convenient to divide the region midway between the electrodes into four annular zones of constant deposition rate, as in Figure 10. In each zone, it will be assumed that the deposition rate is equal to the experimentally determined value at the test point lying inside that zone. Due to the existence of circular symmetry, it is necessary only to consider one quadrant of the electrode, together with the three fibers passing through it. In the calculations presented here, the upper left quadrant was selected.

For each of the three fibers, the overall thickness of plasma polymer deposited can be expressed as

$$S = 2 \sum_{i=1}^{4} \left.\frac{ds}{dt}\right|_i \times \Delta t_i$$

where S is the overall coating thickness, $ds/dt|_i$ is the polymer deposition rate in zone i, and t_i is the time interval that the fiber spends within that zone. The multiplication factor of 2 is required since the fiber also moves through the lower left quadrant.

Δt_i, however, is given by

$$\Delta t_i = l_i/\nu$$

in which l_i is the length of fiber lying in the ith zone, and ν is the fiber feed rate. Hence

$$S = \frac{2}{\nu}\left[\sum_{i=1}^{4} \left.\frac{ds}{dt}\right|_i \times l_i\right]$$

Substituting the values of l_i from Figure 10 into the equation above, one obtains for the three fibers

fiber 1:

$$S = \frac{2}{(\nu \text{ cm/min})}\left[(1.3 \text{ cm})\left.\frac{ds}{dt}\right|_1 + (1.4 \text{ cm})\left.\frac{ds}{dt}\right|_2 + (1.4 \text{ cm})\left.\frac{ds}{dt}\right|_3 + (2.6 \text{ cm})\left.\frac{ds}{dt}\right|_4\right]$$

fiber 2:

$$S = \frac{2}{(\nu \text{ cm/min})}\left[(0.2 \text{ cm})\left.\frac{ds}{dt}\right|_1 + (2.1 \text{ cm})\left.\frac{ds}{dt}\right|_2 + (1.5 \text{ cm})\left.\frac{ds}{dt}\right|_3 + (2.7 \text{ cm})\left.\frac{ds}{dt}\right|_4\right]$$

fiber 3:

$$S = \frac{2}{(\nu \text{ cm/min})}\left[(0)\left.\frac{ds}{dt}\right|_3 + (1.5 \text{ cm})\left.\frac{ds}{dt}\right|_4 + (1.9 \text{ cm})\left.\frac{ds}{dt}\right|_3 + (2.9 \text{ cm})\left.\frac{ds}{dt}\right|_4\right]$$

$ds/dt|_i$ is in Å/min. Table I was obtained by substituting the experimental deposition rates for a range of reaction conditions into the three equations above. The fiber feed rate was taken to be 1.0 cm/min.

Registry No. Poly(pyridine) (homopolymer), 25013-01-8; poly(allylamine) (homopolymer), 30551-89-4.

Literature Cited

Bell, A. T.; Wydeven, T.; Johnson, C. C. *J. Appl. Polym. Sci.* **1975**, *19*, 1911.

Buck, K. R.; Davar, V. K. *Br. Polym. J.* **1970**, *2*, 238.

Cormia, R. L.; Tsujimoto, N. K.; Andresen, S. U.S. Patent 4 013 532, 1977.

Hollahan, J. R.; Wydeven, T. *Science* **1973**, *179*, 500.

Morosoff, N. Preparation of Composite Hollow Fiber Reverse Osmosis Membranes by Plasma Polymerization, Final Report for the Office of Water Research and Technology, Washington, DC, Aug 1978.

Morosoff, N.; Newton, W.; Yasuda, H. *J. Vac. Sci. Technol.* **1978**, *15*(6), 1815.

Peric, D.; Bell, A. T.; Shen, M. *J. Appl. Polym. Sci.* **1977**, *21*, 2661.

Sherwood, T. K.; Brian, P. L. T.; Fisher, R. E.; Dresser, L. *Ind. Eng. Chem. Fundam.* **1985**, *4*, 113.

Yasuda, H.; Lamaze, C. D. *J. Appl. Polym. Sci.* **1973a**, *17*, 201.

Yasuda, H. *J. Appl. Polym. Sci.* **1973b**, *17*, 1533.

Yasuda, H.; Marsh, H. C.; Tsai, J. *J. Appl. Polym. Sci.* **1975**, *19*, 2157.

Yasuda, H.; Marsh, H. C.; Brandt, E. S.; Reilley, C. N. *J. Appl. Polym. Sci.* **1976**, *20*, 543.

Yasuda, H.; Hirotsu, T. *J. Polym. Sci. Polym. Chem. Ed.* **1978**, *16*, 743.

Yasuda, H.; Inagaki, N. *J. Appl. Polym. Sci.* **1981**, *26*, 3557.

Received for review April 1, 1983
Revised manuscript received September 14, 1983
Accepted October 3, 1983